Wang, Wan-Fa; Li, Si-Liang; Zhong, Jun; Maberly, Stephen C.; Li, Cai; Wang, Fu-Shun; Xiao, Hua-Yun; Liu, Cong-Qiang. 2020. **Climatic and anthropogenic regulation of carbon transport and transformation in a karst river-reservoir system.**

The definitive version was published in *Science of the Total Environment*, 707, 135628. https://doi.org/10.1016/j.scitotenv.2019.135628

The definitive version is available at www.elsevier.com/

Climatic and anthropogenic regulation of carbon transport and transformation in a karst river-reservoir system

Wan-Fa Wang[a], Si-Liang Li[a, b]*, Jun Zhong[a], Stephen C. Maberly[c], Cai Li[d], Fu-Shun Wang[e], Hua-Yun Xiao[a, f], Cong-Qiang Liu[a]

[a]Institute of Surface-Earth System Science, Tianjin University, Tianjin 300072, China

[b]State Key laboratory of Hydraulic Engineering Simulation and Safety, Tianjin University, Tianjin 300072, China

[c]Lake Ecosystems Group, NERC Centre for Ecology & Hydrology, Lancaster Environment Centre, Lancaster, UK

[d]School of Urban and Environment Science, Huaiyin Normal University, Huaian 223300, China

[e]School of Environmental and Chemical Engineering, Shanghai University, Shanghai 200433, China

[f]State Key Laboratory of Environmental Geochemistry, Institute of Geochemistry, Chinese Academy of Sciences, Guiyang 550002, China

*Corresponding author: Si-Liang Li

Email: siliang.li@tju.edu.cn

Fax, 0086 22 27405053

Highlights

- DIC concentrations and $\delta^{13}C_{DIC}$ trends were investigated across cascaded reservoirs.
- Carbon dynamics in the reservoirs were mainly impacted by biological processes.
- Damming effect is controlled by both hydraulic retention time and air temperature.
- The damming effect can be weakened by regulating the hydraulic retention time.

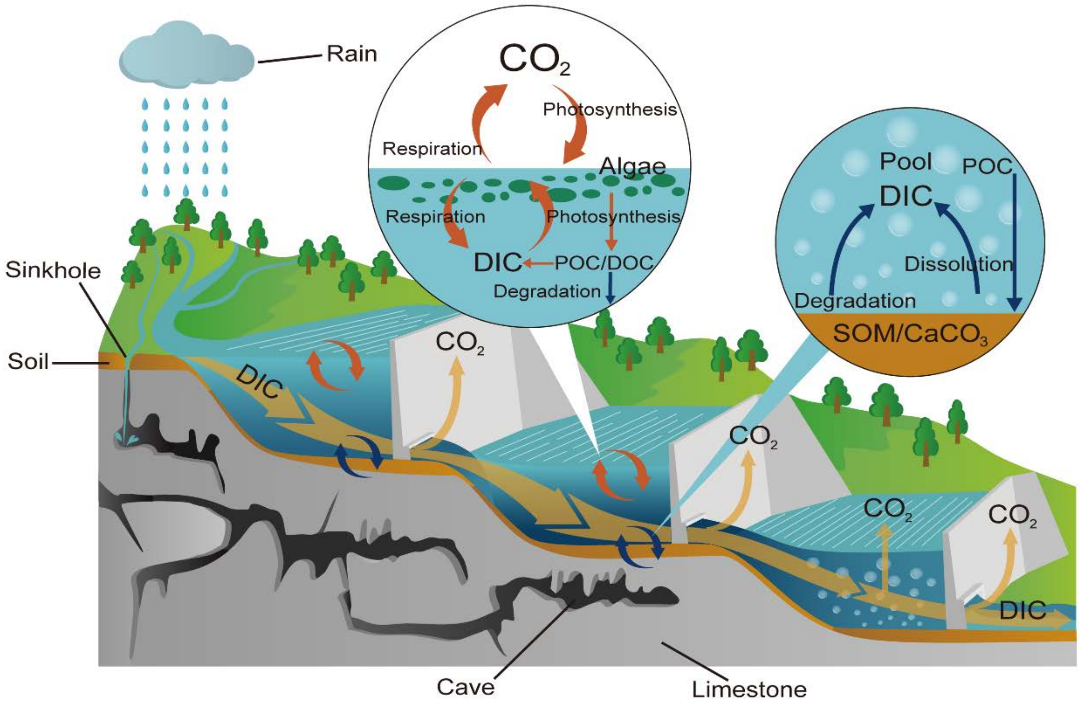
Rain
CO_2
Photosynthesis
Respiration
Algae
Respiration
Photosynthesis
DIC
POC/DOC
Degradation
Pool
POC
DIC
Dissolution
Degradation
SOM/$CaCO_3$
Sinkhole
Soil
DIC
CO_2
CO_2
CO_2
CO_2
DIC
Cave
Limestone

Abstract

The effect of dams on dissolved inorganic carbon (DIC) transport and riverine ecosystems is unclear in karst cascade reservoirs. Here, we analysed water samples from a karst river system with seven cascade reservoirs along the Wujiang River, southwestern China, during one hydrological year. From upstream to downstream, the average concentration of DIC increased from 2.2 to 2.6 mmol/L and its carbon isotope composition ($\delta^{13}C_{DIC}$) decreased from -8.0 to -10‰. Meanwhile, the air temperature (Ta) increased from 20.3°C to 26.7°C and 10°C to 13.7°C in the warm and cold seasons, respectively. The results suggest that a cascade of dams has a stronger effect on DIC dynamics and retention than a single dam. The good correlation between Ta/HRT (hydraulic retention time) and Δ[DIC] as well as $\Delta[\delta^{13}C_{DIC}]$ mean that Ta and HRT affected the magnitude of the damming effect by altering changes in concentration of DIC and $\delta^{13}C_{DIC}$ in the reservoir compared to the inflowing water. In particular, daily regulated reservoirs with short retention times acted more like river corridors and had a smaller effect on carbon dynamics, so modulating retention time might be used reduce the effect of dams on the riverine ecosystem.

Keywords: Dissolved inorganic carbon, Carbon isotope, Damming effect, Cascade reservoirs, Hydraulic retention time

1. Introduction

Damming a river provides numerous goods and services for human society by facilitating the development of agriculture, industry and tourism but can also have adverse effects on the local aquatic environment and the global carbon budget (Arthington et al., 2010; Best, 2018; Richter et al., 2010). Increasingly, rivers are dammed by multiple reservoirs in order to increase water resource utilization and hydropower generation (Kondolf et al., 2014; Shi et al., 2017; Zhou et al., 2018). Globally, 48% of river volume has been moderated and 37% of large rivers (longer >1000 km) remain-flowing in the world (Grill et al., 2015, 2019). While single reservoirs have many environmental consequences, the situation is more complex and potentially severe with cascade reservoirs. Past work has concentrated on the effects of reservoirs on greenhouse gases (Kumar et al., 2019 a,b; Li et al., 2018; Maavara et al., 2019; Raymond et al., 2013; Wang et al., 2014a), the water regime (Wang et al., 2019a), sediment and carbon burial and carbon cycle (Bretier et al., 2019; Kondolf et al., 2018; Maavara et al., 2017; Wang et al., 2019b), water utilization and hydropower generation (Zhou et al., 2018), irrigation pressure and other ecological risks (Finer and Jenkins, 2012; Grill et al., 2015; Li et al., 2017; Nilsson et al., 2005; Van and Maavara, 2016; Watkins et al., 2019). DIC represents the largest fraction of total carbon in most rivers and is transported from the continents to the oceans (Meybeck, 1987; Brunet et al., 2009; McClanahan et al., 2016). As a result of carbonate weathering, the DIC concentration in rivers draining karst areas is significantly higher than that in non-karst areas (Li et al., 2010; Han et al., 2010). With the rising demands for energy, rivers have been dammed by multiple dams in the last two decades and the hydrological environment and ecosystem has been severely influenced (Grill et al., 2019; Best, 2018). However, the effects of karst cascade reservoirs on DIC transport and the global carbon cycle are still not clear.

The dissolution of carbonate rocks in karst areas contributes approximately 0.15 Pg C/yr to carbon dioxide (CO_2) sequestration in the ocean based on the chemistry of the largest rivers in the world (Gaillardet et al., 1999). Thus, chemical weathering in karst catchment areas is an important carbon sink (Beaulieu et al., 2012; Cole et al., 2007; Li et al., 2008; Zeng et al., 2019; Zhong et al., 2018a,b). Southwestern China, with a karst area of about 5.3×10^5 km^2 (Cao et al., 2004), is not only one of the largest karst areas in the world, but also has the most reservoirs in China (Sun et al., 2013). The geomorphology in this area, with narrow and steep river valleys, facilitates the construction of large dams and a series of cascade reservoirs have been created along the major rivers, such as the Wujiang River (Li et al., 2009; Wang et al., 2019a; Zhao et al., 2019), the Jialingjiang River (Cui et al., 2017) and the Yangtze River (Ran et al., 2016; Yang et al., 2005). The damming effect can influence hundreds of kilometers (Finer and Jenkins, 2012), with a huge potential impact on the biogeochemical cycling of inorganic carbon.

The management of a reservoir strongly influences the hydraulic retention time (HRT) of a reservoir along with the water level, water discharge, strength of stratification, and growth of algae. As a key parameter of multi-purpose reservoir operation, HRT is likely to play a critical role in migration and transformation of DIC. In addition, the formation of thermal stratification is strongly influenced by air temperature (Ta). Thermal stratification starts at the end of spring when Ta starts to increase and solar radiation heats the surface water and causes the difference in water density on the vertical column (Menna-Barreto et al., 1969; Elçi, 2008; Zhang et al., 2015). With the variation in Ta, the degree of thermal stratification in the reservoir varies seasonally and geographically. Thus, we hypothesized that HRT and Ta are important factors affecting DIC dynamics in cascade reservoirs. To test this, we analysed the concentration and isotopic composition of DIC ($\delta^{13}C_{DIC}$) in seven cascade reservoirs along the Wujiang River and related these to the characteristics of the reservoirs. Isotopes can be used to trace the migration and transformation of dissolved inorganic carbon in riverine system (Aucour et al., 1999; Li et al., 2008). The results reveal the factors that control DIC dynamics and transport in a typical carbonate dominated cascade of reservoirs.

2. Study area and methods

2.1 Site description

The Wujiang River is the longest tributary of the south bank of the Yangtze River, which is located in the humid subtropical zone and affected by a typical East Asian monsoon climate. From 1957 to 2013, the average annual Ta of the upstream and downstream was 14.1℃ and 17.4℃ and the average annual precipitation was 965 mm and 1125 mm, respectively (Liang et al., 2017). In 2017, the year of this study, the average annual Ta of the upper and lower reaches of the Wujiang River was 15.1℃ and 20.2℃ and the average annual precipitation was 1101.3 mm and 1157.1 mm, respectively (GZPWRD, 2017; CMA, 2019). The total length of the main stream of the Wujiang

River is 1,037 km, with a drop of 2,124 m and a drainage area of 88,267 km^2. The Wujiang River has abundant water resources, and there were eleven cascade hydropower stations along the main stream of the river. The total installed capacity is 10,215 MW, and the annual power generation capacity is 372 MkW·h. In the future, the hydro-power resources will be further developed in the main stream (NDRC, 2018). As the number of dams increases, the river system is further fragmented, which has a significant impact on the regional ecological environment. In order to explore better the damming effect of cascade reservoirs on karst rivers, we selected seven reservoirs (Fig. 1) with different locations and HRT along the main stream. The characteristics of the seven reservoirs are in listed in Table 1.

2.2 Field sampling and data collection

For a comprehensive understanding of the impact of the cascade dams on DIC migration and transformation, a total of 328 water samples from 29 sampling sites were collected in January, April, July and October 2017, including surface water from the inflow, depth-profiles within the reservoir and surface samples from the outflow. Collecting water samples at different depths is helpful to understand the characteristic of the water profile in the lentic area. Generally in these reservoirs, 0-5 m is the epliminion, 5-30 m is the thermocline and below 30 m is the hypolimnion. Thus, surface water was collected from the upper 0.5 m and water for depth-profiles was collected from 0.5, 5, 15, 30, 45 and 60 m. Water temperature (Tw), pH, dissolved oxygen (DO), total dissolved solids (TDS) and chlorophyll (Chl) were measured *in situ* using an automated multiparameter profiler (model YSI EXO) to provide information on the basic hydrochemical characteristics of the water. Total carbonate alkalinity was measured by titration with 0.02 mol/L hydrochloric acid within 12 h using a titrimeter (Brand 4760161). For the analysis of major cations (K^+, Na^+, Ca^{2+} and Mg^{2+}) and dissolved organic carbon (DOC), approximately 50 ml of sample was filtered through 0.45 µm cellulose acetate membrane filters (Whatman, Inc.) and 0.7 µm glass fibre filters (Whatman GF/F), respectively. The filtered water was stored in HDPE bottles at 4℃ in a refrigerator and samples for cations analysis were preserved within 12 h of sampling by adding HNO_3 to keep pH < 2. The major ions and DOC were used to determine ionic strength and characterize the biological activity level, respectively.

2.3 Sample analysis

DOC samples were analyzed using a total organic carbon analyzer (OI Analytical, 1030W), with a detection limit of 0.01mg/L. The analytical error was less than 0.3% based on replicate analysis. Major cations were analyzed using inductively coupled plasma-optical emission spectrometry (ICP-OES), within a relative standard deviation (RSD) of 5%. For $\delta^{13}C_{DIC}$ analysis, 20 ml water was filtered through 0.45 μm PTFE syringe filters, and injected into a vacuumed glass bottle, pre-filled with 2 ml 85% phosphoric acid, at the sampling sites. The CO_2 generated by the reaction was transferred into tubes on a vacuum line and analyzed on a Finnigan MAT 252 mass spectrometer, with an analytical precision of ±0.1‰ (Li et al., 2008). Carbon stable isotope results are expressed in a permil deviation with reference to a standard (PDB). All laboratory analyses were conducted at the Institute of Geochemistry, Chinese Academy of Science (Guiyang, China).

PLS modeling (projections of latent structures by means of partial least squares) was used to identify potential drivers of DIC and $\delta^{13}C_{DIC}$ of the cascade reservoirs, as provided by the software SIMCA-P$^+$ (version 14.1.0.0, Umetrics, Sweden). PLS is widely used because it allows many-to-many linear regression modeling, which can synthesize principal component regression and canonical correlation analysis, can overcome the negative influence of small numbers of sample and the existence of multiple collinearity among variables and maximize the information in raw data to explain dependent variables and improve prediction accuracy (Paranaiba et al., 2018; Peter et al., 2014). The PLS model performance is expressed by R^2Y (explained variance) and by Q^2 (predictive power estimated by cross validation). R^2Y is the model's ability to explain the Y-axis, and Q^2 is the model's prediction ability. The closer R^2Y and Q^2 are, the more stable and reliable is the model. Normally, when $Q^2>0.5$ the model is stable and reliable (Umetrics, 2008). Variable importance in projection (VIP) describes how much a variable contributes to explaining the Y variable and reflects the correlation of the terms to all the responses. The VIP values indicate the relative importance of the variables, highly important variables have VIP>1.0, moderately important variables have VIP 0.8-1.0, and unimportant variables have VIP<0.8. Coefficients and intercepts correspond to, and are analogous to, the slopes and intercepts in an ordinary multiple linear regression. PLS models were validated by comparing goodness of fit of the Y variables. For all statistical tests, the level of significance was taken as $P<0.05$.

2.4 Calculations

The concentration of CO_2 was calculated from pH, alkalinity and temperature and Henry's law was used to convert this to partial pressure of carbon dioxide (pCO_2) with the following equation: $pCO_2 = [H_2CO_3^*]/KCO_2$, where $H_2CO_3^*$ (mol/L) is the sum of hydrated CO_2 (aq) and KCO_2 is Henry's constant for CO_2 at a given temperature (Barth and Veizer, 1999; Neal et al., 1998; Raymond et al., 1997).

DIC concentrations and $\delta^{13}C_{DIC}$ showed significant spatial and temporal variability along the cascade dams (Figs 2 and 3). In order to reveal the major influencing factors and processes related to DIC migration and transformation in cascade reservoirs, we used the inflow water as the reference value to calculate the changing degree of profile water and outflow water samples, which reflected the strength of the reservoir effect. It is defined by the following equations.

$$\Delta[\delta^{13}C_{DIC}] = 100 \times (\delta^{13}C_{DIC}\text{ (sample)}-\delta^{13}C_{DIC}\text{ (inflow)}) /\delta^{13}C_{DIC}\text{ (inflow) (\%)} \quad (1)$$

$$\Delta[DIC] = 100 \times ([DIC](sample)-[DIC]\ (inflow)) /[DIC](inflow)\ (\%) \quad (2)$$

$$\Delta[Tw] = 100 \times ([Tw](sample)-[Tw](inflow)) /[Tw](inflow)\ (\%) \quad (3)$$

Where Δ[DIC], $\Delta[\delta^{13}C_{DIC}]$ and Δ[Tw] represent the % change of $\delta^{13}C_{DIC}$, DIC and water temperature in depth-profiles and outflow waters compared with inflow waters. Δ[Tw] is linked to the thermal stratification capacity, i.e., the higher the Δ[Tw], the stronger the stratification.

3. Results

3.1 Longitudinal variations of water chemical parameters and $\delta^{13}C_{DIC}$ in the surface water

Longitudinal variation in surface Tw, pH, Chl, DO, TDS and Ca^{2+} concentration are shown in Fig. S1, and Ta is shown in Fig. S2 for the study year. The Tw and Ta ranged from 13.1℃ to 31.2℃ (mean = 19.3 ± 4.1℃) and 5.5℃ to 35.3℃ (mean = 18.3 ± 2.1℃), respectively. The pH values ranged from 7.3 to 9.3. They were obviously higher in the reservoir area and the average value was much larger than the discharge water except for in the downstream reservoirs. The concentrations of Chl varied from 0 μg/L to 23.9 μg/L (mean = 4.0 ± 5.4 μg/L) and the variations of DO are from 4.3 mg/L to 19.9 mg/L (mean = 9.2 ± 2.6 mg/L). The water TDS values decreased from upstream to downstream, ranged from 191 mg/L to 334 mg/L, with a mean value of 257 ± 28 mg/L. The Ca^{2+} accounted for 62% to 80% of the total cations, ranging from 36.4 mg/L to 81.5 mg/L (mean = 58.3 ± 7.9 mg/L). All the water chemical parameters mentioned above in the lentic area were larger than those of the inflow and outflow water. These parameters tended to be less variable downstream compared to upstream.

Since pH ranged from 7.3 to 9.3, bicarbonate (HCO_3^-) was the dominant species (>80%) of DIC (Wang et al., 2014b). Therefore, DIC concentrations were expressed as HCO_3^- in this paper. The DIC concentration, DOC concentration and pCO$_2$ values in the surface water increased and then decreased along the river, ranging from 1 to 3.4 mmol/L, 0.6 to 2.7 mg/L and 56 to 9902 μatm, respectively (Fig. 2a, b, c). The $\delta^{13}C_{DIC}$ values in the surface water ranged from -11.5‰ to -1.9‰ (mean = -8.8 ± 2‰) with seasonal variations and in the middle and upper reaches of the reservoir, the average $\delta^{13}C_{DIC}$ values decreased to different degrees after it had passed through a reservoir. The overall trend was a cascade decline from upstream to downstream (Fig. 2d). The mean values of $\delta^{13}C_{DIC}$, pH, DO and Ca^{2+} were the lowest, while the DIC concentrations and pCO$_2$ were the highest in the outflow waters of SL reservoir (Figs 2 and S1). However, the HRT of SL reservoir is less than that of HJD, DF and WJD reservoirs (Table 1).

3.2 Seasonal and vertical variations of DIC and $\delta^{13}C_{DIC}$ down the water column

DIC concentrations and $\delta^{13}C_{DIC}$ values showed significant seasonal variation in the depth profiles, from 1 to 3.6 mmol/L and -12.1 to -1.9‰, respectively. In the warm season, thermal stratification was observed in the reservoirs except for daily regulated reservoirs (SFY, PS and YP). While in the cold seasons with no significant stratification, DIC concentrations and $\delta^{13}C_{DIC}$ varied little in the profiles (Fig. 3). In the depth-profiles, the DIC concentrations increased and $\delta^{13}C_{DIC}$ decreased markedly in the thermocline (0 – 15 m), and became stable in the hypolimnion. Changes in the depth-profiles of daily regulating reservoirs (SFY, PS and YP) were small or absent (Fig. 3). However, in reservoirs with longer HRT, water at depth had high DIC and CO_2 concentrations and the water released from the bottom of the reservoir had a high pCO$_2$ (Fig. 3), which may increase the potential of cascade reservoirs to become CO_2 sources.

3.3 Relationships between DIC, $\delta^{13}C_{DIC}$ and other chemical parameters

Compared to a river, the artificial storage of a reservoir increases HRT, permits thermal stratification and eventually causes a series of changes in water chemical parameters such as Tw, pH, DO, TDS, Chl, DIC, DOC, pCO$_2$, etc. In order to intuitively explore the factors controlling of

DIC, we used PLS to identify potential drivers of DIC and $\delta^{13}C_{DIC}$. In the PLS model, R^2Y are 0.91/0.84, Q^2 are 0.86/0.72, for DIC/$\delta^{13}C_{DIC}$, indicating a high predictive power in this study (Table 2). PLS analyses revealed that Ta, pH, Chl, DO, HRT, Depth and DOC (variable importance in projection, VIP > 0.8; Table 2) were positively associated with DIC or $\delta^{13}C_{DIC}$ (Table 2), while other parameters had a minor influence on DIC concentration and $\delta^{13}C_{DIC}$ (most VIP< 0.8; Table 2).

In order to compare and analyze the data with other reservoirs in karst area, we collected data on DIC concentrations and $\delta^{13}C_{DIC}$ from karst reservoirs with different HRT and annual average Ta published in the Jialing River (JLR) (Cui et al., 2017), Bajiangkou reservoir of Zhujiang River (ZJR) (Tang et al., 2014), Puding reservoir of Sancha River (SCR) (Qian et al., 2017) and cascade reservoirs in Maotiao River (MTR) (Li et al., 2009). Detailed data and discussion are given in the Discussion.

4. Discussion

4.1 Influence of HRT and environmental factors on DIC variation

The DIC in karst rivers mainly originates from carbonate weathering (Han et al., 2010; Li et al., 2008). However, the altered hydrodynamics in reservoirs can change the processes controlling DIC concentrations and $\delta^{13}C_{DIC}$ values compared to similar areas without dams (Li et al., 2010; Zhong et al., 2017, 2018b). For example, reservoirs in this study area usually discharge water from the bottom of their dam, and since thermal stratification occurs in reservoirs with long HRT in the warm season (Wang et al., 2019c), a series of internal hydrochemical changes can occur, which is responsible for the increase in DIC concentrations and decrease in $\delta^{13}C_{DIC}$ values (Fig. 3, Fig. S3).

From the upstream to the downstream areas, the concentration of DIC gradually increased both in the surface and along the water profiles and reached a maximum at SL reservoir, while it tended to be stable in the downstream due to the non-thermal stratification. With the increase of DIC concentrations, $\delta^{13}C_{DIC}$ values gradually decreased, indicating that longer HRT and high air temperature promoted the formation of thermal stratification and enhanced biochemical reactions, such as the photosynthesis of surface algae and the degradation of bottom organic matter (Han et al., 2018; Wang et al., 2019c).

We used both Δ[DIC] and Δ[$\delta^{13}C_{DIC}$] to analyse these processes transforming DIC in these cascade reservoirs (Alling et al., 2012; Samanta et al., 2015; Wang et al., 2019c). Fig. 4 shows that DIC is affected by different processes at different depths including biological production, outgassing, carbonate precipitation and dissolution, and degradation of DOC and particulate organic carbon (POC). The analysis shows that biological production and CO_2 outgassing are the dominant processes in the surface of the reservoirs while the degradation of organic carbon dominates at depth (Fig. 4). There are three major sources of POC in the river-reservoir system: (i) terrestrial plants from the basin. The average $\delta^{13}C$ of terrestrial C3 plants and C4 plants are −32‰ to −24‰ and −13‰ to −10‰, respectively (Kohn, 2010; Cerling et al., 1997). From the previous study, riverine POC in the study area is mainly from terrestrial C3 plant debris, and the average $\delta^{13}C_{POC}$ is about −28‰ (Han et al., 2018); (ii) Aquatic phytoplankton. The $\delta^{13}C$ of freshwater phytoplankton ranges from −34.4‰ to −5.9‰ (Vuorio et al., 2006); (iii) Microbial biomass. Microbes have a mean value of $\delta^{13}C$ of about −55‰ (Freeman et al., 1990). Reservoir DOC is also influenced by the above three sources. High DOC concentrations in the epilimnion derive from terrestrial organic matter (OM) and the release by phytoplankton. DOC concentrations decreased and DIC increased with the increase of water depth by photodegradation in the euphotic zone and microbial degradation in the profile and sediment (Shi et al., 2017; Teodoru et al, 2013; Tranvik et al., 2009).

Seasonal stratification in the warm season enhances algal photosynthesis in the euphotic layer, consuming CO_2 and HCO_3^- and leading to a decreased DIC concentration (Maberly, 1996; Zhao et al., 2019). The OM produced by phytoplankton would enter into the bottom of the reservoir when the water column overturned (f1 in Fig. 4). The carbon:nitrogen (C:N) ratio, is a natural tracer identifying POC provenance in riverine environments and varies from 14 to 50 in plant OM (C3 and C4) and 5 to 8 in phytoplankton (Ogrinc et al. 2008; Liu et al., 2018). The molar C:N ratio ranged from 4.7 to 8.9 (average = 6.6) in POC from the Maotiao cascade reservoirs of the Wujiang River (Liu et al., 2018). This indicates that autochthonous OM is an important component of organic matter in sediments, which is responsible for the variation of DIC with allochthonous terrestrial plant OM in the reservoirs (Wang et al., 2019b).

In addition, photosynthesis can increase pH and cause calcium carbonate precipitation (Chen and Liu, 2017; Millo et al., 2012; Vuorio et al., 2006) (f2) and accelerate the decomposition of POC and DOC in the bottom region (f3) (Kumar et al., 2019b; Wang et al., 2019c). A ^{14}C tracer method also showed that the presence of $CaCO_3$ in the sediment would affect the condition of soil aggregates and pH and promote the decomposition of organic matter (Motavalli et al., 1995). The decrease of pH caused by anaerobic decomposition of organic matter at the bottom of the reservoir would produce CO_2, increasing DIC and also lead to a further increase of DIC content by calcium carbonate decomposition (f4), and finally lead to an increase of DIC content discharged from the reservoir bottom area. However, the degradation of organic matter is dominant in this area as indicated by the depletion of ^{13}C in the bottom region (Han et al., 2018; Wang et al., 2019c). DIC generated at the bottom of the reservoir will further promote the photosynthesis of surface water downstream of the reservoir via discharged water (f5, f6), and provide support for the degradation of organic matter (equation 4) at the bottom (Wang et al., 2019b; Lu et al., 2018).

$$CaCO_3+CO_2+H_2O \leftrightarrow HCO_3^-+Ca^{2+} \rightarrow \text{(Photosynthesis) } CaCO_3\downarrow+x(CO_2\uparrow+H_2O)+(1-x)(CH_2O\downarrow+O_2\uparrow) \quad (4)$$

Finally, these effects (equation 4) would jointly promote the decomposition of organic matter to form DIC and transfer to the downstream of the river. Compared to other reservoirs, the average concentration of DIC (2.92 mmol/L) and the average value of $\delta^{13}C_{DIC}$ (-10.6‰) in the discharged water were the maximum and minimum values, respectively in SL reservoir (Fig. 3). However, SL reservoir is only a monthly regulated reservoir, with a lower HRT (22 days) than that of HJD (368 days), WJD (49 days) and DF (29 days). Compared with the inflow water, the variation in the degree of $\delta^{13}C_{DIC}$ was also greater than that of the DF and WJD reservoirs. In addition, the DIC concentration and $\delta^{13}C_{DIC}$ in the discharged water showed spatial variability along the cascade reservoirs. Therefore, HRT may not be the only factor controlling the migration and transport of DIC.

4.2 The factors controlling DIC in river-reservoir systems

Air temperature is an important factors linked to the stratification of the reservoir and biological components (Elçi, 2008; Feuchtmayr et al., 2019; Zhang et al., 2015). The normal elevation of SL reservoir is 440 m, which is much lower than that of HJD (1140 m), resulting in an average Ta difference of 6.3°C between the two reservoirs in the warm season. VIP values (1.35 /1.45) in the PLS model indicate (Table 2) that average Ta has the highest correlation with DIC concentrations and $\delta^{13}C_{DIC}$ values, so we speculate that Ta may play an important role in DIC geochemical behavior and transport by influencing reservoir stratification. The contour maps of the DIC and $\delta^{13}C_{DIC}$ in the cascade reservoirs (Fig. S4), suggest that the higher Ta under the same residence time conditions, the higher were the DIC concentration and the more negative were the $\delta^{13}C_{DIC}$ values. This indicates that different HRT and Ta can cause complex processes in the reservoirs and affect the DIC behavior.

In order to test our hypothesis and clarify the influence of average Ta and HRT on DIC transport, we fitted the relationship diagram of Ta/HRT with Δ[DIC] and $\Delta[\delta^{13}C_{DIC}]$ (Fig. 5). The patterns were consistent with the trend predicted in Fig. S4: when the retention time was constant, the concentrations of DIC increased with Ta, indicating that Ta affected the stability of reservoir stratification and finally accelerated the degradation of organic matter in the hypolimnion. This also explains why DIC concentrations and $\delta^{13}C_{DIC}$ varies greatly in the SL reservoir despite a short HRT because of the higher Ta. The strong damming effect ultimately can cause more CO_2 to be released downstream, especially during monsoon and post-monsoon periods when the air temperature is high and stratification is strong with degradation of organic carbon occurring in the water at depth, reflecting the processes that occur in lakes (Kumar et al., 2018; Maberly et al., 2013; Shi et al., 2017), which is characterized by lower $\delta^{13}C_{DIC}$ and more DIC contributed to the retention effect (Figs 3 and 5). However, in the cold season, as the Ta decreases, the thermal stratification of the water weakens. The increase of DO in the column will accelerate the decomposition of OM in the sediment (Teodoru et al, 2013; Tranvik et al., 2009; Mcclanahan et al., 2016; Zhao et al., 2019), causing the increase in DIC concentrations and decrease in $\delta^{13}C_{DIC}$ in the column, which is different from the warm season when reservoirs with longer HRT have an opposite trend of DIC concentrations and $\delta^{13}C_{DIC}$ in the water column caused by thermal stratification (Wang et al., 2019c; Tranvik et al., 2009; Vuorio et al., 2006).

Our study showed that the DIC concentration and its isotopic values were mainly dependent on the Ta and HRT in the Wujiang cascade reservoirs and other karst reservoirs. It indicates that the altitude of each reservoir in different cascade reservoirs affects the regional climate, which will affect the carbon cycle to varying degrees due to artificial regulation (Fig. 6). We can infer that:

(1) In the same climatic zone, the DIC concentrations of the inflow water is taken as the initial

value, and we assume that the increased DIC would return to the initial value by outgassing CO_2. In this study, the mean value of $\delta^{13}C_{DIC}$ was -10.4‰ in the downstream, which was similar to the mean $\delta^{13}C_{DIC}$ of -9.7‰ in the karst river catchment with no dam (Li et al., 2010). Therefore, although there are reservoirs downstream, the damming effect is weak in the daily regulated reservoirs and gradually returns to the state of a river. Thus, by reducing the HRT to a daily regulating reservoir (<7 day), the CO_2 emissions from the discharge water with a HRT >7 days will be reduced by about 2%-12%, calculated based on the variation of $p$$CO_2$ values from the seven reservoirs in this study (Fig. 2).

(2) In the same geological lithology area, when the HRT is consistent, every 1℃ increase in Ta will elevate DIC concentrations by ~6% compared to the inflow water. However, the damming effect is more pronounced in the reservoirs with higher Ta. In the case of Silin reservoir (HRT = 22 day) in the downstream, due to the high Ta in the warm season, once the water body forms stable thermal stratification, even if the HRT is short the $p$$CO_2$ in the discharge water is 1.6 times and 2.3 times that of the Hongjiadu reservoir (HRT = 368 day) and the Wujiangdu reservoir (HRT = 49 day) in the upstream and downstream, respectively.

(3) Our data, model and results can play a critical part in evaluating the impact of cascade dams on the carbon cycle, and our study is also a new perspective for identifying the damming effect of different reservoir types in the cascade reservoirs. It can also provide a scientific basis for weakening damming effects, such as reducing greenhouse gas emissions, improving water quality by artificial regulation and help address the ecological risks.

5. Conclusions

Cascade dams on a river can alter riverine DIC concentrations and $\delta^{13}C_{DIC}$ by altering the geochemistry of a river through variations of HRT and Ta. Along the Wujiang River, DIC concentrations increased downstream while $\delta^{13}C_{DIC}$ showed a converse trend, indicating that the retention effect of the DIC gradually increased from the upstream to the downstream. Moreover, the damming effect may depend on the interaction between HRT and Ta. Reservoirs with a long HRT and high Ta had a large effect on DIC dynamics. In this study, we found that the "hot spot" reservoir like SL, where the HRT is not long, whereas the damming effect is stronger than other reservoirs with longer HRT and lower Ta. Given its higher carbon emission, the reservoirs incurred a greater global warming effect among the cascade reservoirs, which is enhanced by the long HRT and high Ta. In addition, we are also surprised to find that even in reservoirs with higher Ta like PS and YP, the damming effect is weak with the short HRT. Therefore, the results of our research emphasize the need to frame reservoir management in a truly multidisciplinary context and consider reducing CO_2 emissions by managing HRT.

Conflict of interest

The authors declare that they have no competing financial interest associated with this work.

Acknowledgments

This work was supported by the National Key R&D Program of China under Grant No. 2016YFA0601002, National Natural Science Foundation of China under Grant No. 41571130072. The authors are grateful to Prof. Baoli Wang and Xiaodong Li for their help in the field work. The authors would like to thank Prof. Philippe Van Cappellen from the University of Waterloo for the discussion. We also thank Yuanbi Yi, Sainan Chen, Mengdi Yang and Xiaolong Qiu for helping in the field. We are grateful to the editor and reviewers for their constructive comments.

References

Abril, G., Etcheber, H., Delille, B., Frankignoulle, M., Borges, A.V., 2003. Carbonate dissolution in the turbid and eutrophic Loire estuary. Mar. Ecol.-Prog. 259, 129-138. https://doi.org/10.3354/meps259129.

Alling, V., Porcelli, D., Mörth, C.M., Anderson, L.G., Sanchez-Garcia, L., Gustafsson, Ö., Andersson, P.S., Humborg, C., 2012. Degradation of terrestrial organic carbon, primary production and out-gassing of CO_2 in the Laptev and East Siberian Seas as inferred from $\delta^{13}C$ values of DIC. Geochim. Cosmochim. Acta. 95, 143-159. https://doi.org/10.1016/j.gca.2012.07.028.

Arthington, A.H., Naiman, R.J., McClain, M.E., Nilsson, C., 2010. Preserving the biodiversity and ecological services of rivers: new challenges and research opportunities. Freshw. Biol. 55, 1-16. https://doi.org/10.1111/j.1365-2427.2009.02340.x.

Aucour, A.M., Sheppard, S.M.F., Guyomar, O., Wattelet, J., 1999. Use of ^{13}C to trace origin and cycling of inorganic carbon in the Rhône river system. Chem. Geol. 159, 87-105. https://doi.org/10.1016/S0009-2541(99)00035-2.

Barth, J.A.C., Veizer, J., 1999. Carbon cycle in St. Lawrence aquatic ecosystems at Cornwall (Ontario), Canada: seasonal and spatial variations. Chem. Geol. 159, 107-128.

https://doi.org/10.1016/S0009-2541(99)00036-4.

Beaulieu, E., Goddéris, Y., Donnadieu, Y., Labat, D., Roelandt, C., 2012. High sensitivity of the continental-weathering carbon dioxide sink to future climate change. Nat. Clim. Chang. 2, 346-349. https://doi.org/10.1038/nclimate1419.

Best, J., 2018. Anthropogenic stresses on the world's big rivers. Nat. Geosci. 12, 7-21. https://doi.org/10.1038/s41561-018-0262-x.

Bretier, M., Dabrin, A., Bessueille-Barbier, F., Coquery, M., 2019. The impact of dam flushing event on dissolved trace elements concentrations: Coupling integrative passive sampling and discrete monitoring. Sci. Total Environ. 656, 433-446. https://doi.org/10.1016/j.scitotenv.2018.11.303.

Brunet, F., Dubois, K., Veizer, J., Nkoue Ndondo, G.R., Ndam Ngoupayou, J.R., Boeglin, J.L., Probst, J.L., 2009. Terrestrial and fluvial carbon fluxes in a tropical watershed: Nyong basin, Cameroon. Chemical Geology. 265, 563-572. https://doi.org/10.1016/j.chemgeo.2009.05.020.

Cerling, T.E., Harris, J.M., MacFadden, B.J., Leakey, M.G., Quade, J., Eisenmann, V., Ehleringer, J.R., 1997. Global vegetation change through the Miocene/Pliocene boundary. Nature. 389, 153-158. https://doi.org/10.1038/38229.

Chen, C.Y., Liu, Z.H., 2017. The role of biological carbon pump in the carbon sink and water environment improvement in karst surface aquatic ecosystems. Chin. Sci. Bull. 62, 3440-3450. https://doi.org/10.1360/n972017-00298.

CMA, China Meteorological Administration, 2017. http://www.cma.gov.cn/, Accessed data: 1 January 2017 to 31 December 2017

Cole, J.J., Prairie, Y.T., Caraco, N.F., McDowell, W.H., Tranvik, L.J., Striegl, R.G., Duarte, C.M., Kortelainen, P., Downing, J.A., Middelburg, J.J., Melack, J., 2007. Plumbing the Global Carbon Cycle: Integrating Inland Waters into the Terrestrial Carbon Budget. Ecosystems. 10, 171-184. https://doi.org/10.1007/s10021-006-9013-8.

Cui, G.Y., Li, X.D., Li, Q.K., Huang, J., Tao, Y.L., Li, S.Q., Zhang, J., 2017. Damming effects on dissolved inorganic carbon in different kinds of reservoirs in Jialing River, Southwest China. Acta Geochim. 36, 581-597. https://doi.org/10.1007/s11631-017-0155-5.

Elçi, Ş., 2008. Effects of thermal stratification and mixing on reservoir water quality. Limnology. 9, 135-142. https://doi.org/10.1007/s10201-008-0240-x.

Feuchtmayr, H., Pottinger, T.G., Moore, A., De Ville, M.M., Caillouet, L., Carter, H.T., Pereira, M.G., Maberly, S.C., 2019. Effects of brownification and warming on algal blooms, metabolism and higher trophic levels in productive shallow lake mesocosms. Sci. Total Environ. 678, 227-238. https://doi.org/10.1016/j.scitotenv.2019.04.105.

Freeman, K.H., Hayes, J.M., Trendel, J.-M., Albrecht, P., 1990. Evidence from carbon isotope measurements for diverse origins of sedimentary hydrocarbons. Nature. 343, 254-256. https://doi.org/10.1038/343254a0.

Finer, M., Jenkins, C.N., 2012. Proliferation of hydroelectric dams in the Andean Amazon and implications for Andes-Amazon connectivity. PLoS One. 7, e35126. https://doi.org/10.1371/journal.pone.0035126.

Gaillardet, J., Dupré, B., Louvat, P.l., Allegre, C.J., 1999. Global silicate weathering and CO_2

consumption rates deduced from the chemistry of large rivers. Chem. Geol. 159, 3-30. https://doi.org/10.1016/s0009-2541(99)00031-5.

Grill, G., Lehner, B., Lumsdon, A.E., MacDonald, G.K., Zarfl, C., Reidy Liermann, C., 2015. An index-based framework for assessing patterns and trends in river fragmentation and flow regulation by global dams at multiple scales. Environ. Res. Lett. 10, 015001. https://doi.org/10.1088/1748-9326/10/1/015001.

Grill, G., Lehner, B., Thieme, M., Geenen, B., Tickner, D., Antonelli, F., Babu, S., Borrelli, P., Cheng, L., Crochetiere, H., Ehalt Macedo, H., Filgueiras, R., Goichot, M., Higgins, J., Hogan, Z., Lip, B., McClain, M.E., Meng, J., Mulligan, M., Nilsson, C., Olden, J.D., Opperman, J.J., Petry, P., Reidy Liermann, C., Sáenz, L., Salinas-Rodríguez, S., Schelle, P., Schmitt, R.J.P., Snider, J., Tan, F., Tockner, K., Valdujo, P.H., van Soesbergen, A., Zarfl, C., 2019. Mapping the world’s free-flowing rivers. Nature. **569**(7755), 215-221. https://doi.org/10.1038/s41586-019-1111-9.

GZPWRD, water resources bulletin of Guizhou Province, 2017. Water resources department of Guizhou province. http://www.gzmwr.gov.cn/, Accessed date: 15 January 2019.

Han, G.L., Tang, Y., Xu, Z.F., 2010. Fluvial geochemistry of rivers draining karst terrain in Southwest China. Journal of Asian Earth Sciences. 38, 65-75. https://doi.org/10.1016/j.jseaes.2009.12.016.

Han, Q., Wang, B.L., Liu, C.Q., Wang, F.S., Peng, X., Liu, X.L., 2018. Carbon biogeochemical cycle is enhanced by damming in a karst river. Sci. Total Environ. 616, 1181-1189. https://doi.org/10.1016/j.scitotenv.2017.10.202.

Kondolf, G.M., Rubin, Z.K., Minear, J.T., 2014. Dams on the Mekong: cumulative sediment starvation. Water Resour. Res. 50, 5158-5169. https://doi.org/10.1002/2013wr014651.

Kondolf, G.M., Schmitt, R.J.P., Carling, P., Darby, S., Arias, M., Bizzi, S., Castelletti, A., Cochrane, T.A., Gibson, S., Kummu, M., Oeurng, C., Rubin, Z., Wild, T., 2018. Changing sediment budget of the Mekong: Cumulative threats and management strategies for a large river basin. Sci. Total Environ. 625, 114-134. https://doi.org/10.1016/j.scitotenv.2017.11.361.

Kohn, M.J., 2010. Carbon isotope compositions of terrestrial C3 plants as indicators of (paleo) ecology and (paleo) climate. Proc Natl Acad Sci U S A. 107, 19691-19695. https://doi .org/10.2307/25748741.

Kumar, A., Sharma, M.P., Yang, T., 2018. Estimation of carbon stock for greenhouse gas emissions from hydropower reservoirs. Stoch. Environ. Res. Risk Assess. 32, 3183-3193. https://doi.org/10.1007/s00477-018-1608-z.

Kumar, A., Yang, T., Sharma, M.P., 2019a. Greenhouse gas measurement from Chinese freshwater bodies: A review. J. Clean Prod. 233, 368-378. https://doi.org/10.1016/j.jclepro.2019.06.052.

Kumar, A., Yang, T., Sharma, M.P., 2019b. Long-term prediction of greenhouse gas risk to the Chinese hydropower reservoirs. Sci. Total Environ. 646, 300-308. https://doi.org/10.1016/j.scitotenv.2018.07.314.

Li, G.R., Liu, C.Q., Chen, C., Wang, B.L., Li, J., Li, S.L., Liu, X.L., Wang, F.S., 2009. Dissolved inorganic carbon and its carbon isotope composition in cascade reservoir of the Maotiao River during summer and autumn. Environ Sci. 30, 2891-2897 (in Chinese).

Li, S.L., Calmels, D., Han, G.L., Gaillardet, J., Liu, C.Q., 2008. Sulfuric acid as an agent of carbonate weathering constrained by $\delta^{13}C_{DIC}$: Examples from Southwest China. Earth Planet. Sci. Lett. 270, 189-199. https://doi.org/10.1016/j.epsl.2008.02.039.

Li, S.L., Liu, C.Q., Li, J., Lang, Y.C., Ding, H., Li, L.B., 2010. Geochemistry of dissolved inorganic carbon and carbonate weathering in a small typical karstic catchment of Southwest China: Isotopic and chemical constraints. Chem. Geol. 277, 301-309. https://doi.org/10.1016/j.chemgeo.2010.08.013.

Li, S.Y., Bush, R.T., Santos, I.R., Zhang, Q., Song, K., Mao, R., Wen, Z., Lu, X.X., 2018. Large greenhouse gases emissions from China's lakes and reservoirs. Water Res. 147, 13-24. https://doi.org/10.1016/j.watres.2018.09.053.

Li, Z., Lu, L.H., Lv, P.Y., Du, H.L., Guo, J.S., He, X., Ma, J.R., 2017. Carbon footprints of pre-impoundment clearance on reservoir flooded area in China's large hydro-projects: Implications for GHG emissions reduction in the hydropower industry. J. Clean Prod. 168, 1413-1424. https://doi.org/10.1016/j.jclepro.2017.09.091.

Liang, L., Zhang, H.X., Huang, W., 2017. Analysis of climate change characteristics of cascade reservoirs in the main stream of the Wujiang River. Yangtze River. 48, 68-72 (in Chinese).

Liu, X.L., Li, S.L., Wang, Z.L., Wang, B.L., Han, G.L., Wang, F.S., Bai, L., Xiao, M., Yue, F.J., Liu, C.Q., 2018. Sources and key processes controlling particulate organic nitrogen in impounded river–reservoir systems on the Maotiao River, southwest China. Inland Waters. 8, 167-175. https://doi.org/10.1080/20442041.2018.1462612.

Lu, W.Q., Wang, S.L., Yeager, K.M., Liu, F., Huang, Q.S., Yang, Y.X., Xiang, P., Lü, Y.C., Liu, C.Q., 2018. Importance of Considered Organic Versus Inorganic Source of Carbon to Lakes for Calculating Net Effect on Landscape C Budgets. Journal of Geophysical Research: Biogeosciences. 123, 1302-1317. https://doi.org/10.1002/2017JG004159.

Maavara, T., Lauerwald, R., Laruelle, G.G., Akbarzadeh, Z., Bouskill, N.J., Van Cappellen, P., Regnier, P., 2019. Nitrous oxide emissions from inland waters: Are IPCC estimates too high? Glob. Change Biol. 25, 473-488. https://doi.org/10.1111/gcb.14504.

Maavara, T., Lauerwald, R., Regnier, P., Van Cappellen, P., 2017. Global perturbation of organic carbon cycling by river damming. Nat. Commun. 8, 1-10. https://doi.org/10.1038/ncomms15347.

Maberly, S.C., Barker, P.A., Stott, A.W., De Ville, M.M., 2013. Catchment productivity controls CO_2 emissions from lakes. Nat. Clim. Chang. 3, 391-394. https://doi.org/10.1038/nclimate1748.

Maberly, S.C., 1996. Diel, episodic and seasonal changes in pH and concentrations of inorganic carbon in a productive lake. Freshw. Biol.. 35, 579-598. https://doi.org/10.1111/j.1365-2427.1996.tb01770.x.

Menna Barreto, S.S., Fontoura, M.A., Lemes, E.T., Freitas, F.M., Ferraz, S.C., Silva, E.D., Corrêa, C.L., 1969. Thermal stratification in lakes: Analytical and laboratory studies. Water Resour. Res. 5, 484–495. https://doi.org/10.1029/wr005i002p00484.

Meybeck, M., 1987. Global chemical weathering of surficial rocks estimated from river dissolved loads. Am. J. Sci. 287, 401-428. https://doi.org/10.2475/ajs.287.5.401.

Mcclanahan, K., Polk, J., Groves, C., Osterhoudt, L., Grubbs, S., 2016. Dissolved inorganic carbon sourcing using $\delta^{13}C_{DIC}$ from a karst influenced river system. Earth Planet. Sci. Lett. 41, 392-

405. https://doi.org/10.1002/esp.3856.

Millo, C., Dupraz, S., Ader, M., Guyot, F., Thaler, C., Foy, E., Ménez, B., 2012. Carbon isotope fractionation during calcium carbonate precipitation induced by ureolytic bacteria. Geochim. Cosmochim. Acta. 98, 107-124. https://doi.org/10.1016/j.gca.2012.08.029.

Motavalli, P.P., Palm, C.A., Parton, W.J., Elliott, E.T., Frey, S.D., 1995. Soil pH and organic C dynamics in tropical forest soils: Evidence from laboratory and simulation studies. Soil Biol. Biochem. 27, 1589-1599. https://doi.org/10.1016/0038-0717(95)00082-p.

NDRC. 2018. Reply of the State Development and Reform Commission on the approval of Chongqing Wujiang White Horse Electric Navigation Hub Project. http://zfxxgk.nea.gov.cn/auto87/201804/t20180412_3142.htm, Accessed date: 20 March 2019 (in chinese).

Neal, C., House, W.A., Down, K., 1998. An assessment of excess carbon dioxide partial pressures in natural waters based on pH and alkalinity measurements. Sci. Total Environ. 210, 173-185. https://doi.org/10.1016/s0048-9697(98)00011-4.

Nilsson, C., Reidy, C.A., Dynesius, M., Revenga, C., 2005. Fragmentation and flow regulation of the world's large river systems. Science. 308, 405-408. https://doi.org/10.1126/science.1107887.

Ogrinc, N., Markovics, R., Kanduč, T., Walter, L.M., Hamilton, S.K., 2008. Sources and transport of carbon and nitrogen in the River Sava watershed, a major tributary of the River Danube. Applied Geochemistry. 23, 3685-3698. https://doi.org/10.1016/j.apgeochem.2008.09.003.

Paranaiba, J.R., Barros, N., Mendonca, R., Linkhorst, A., Isidorova, A., Roland, F., Almeida, R.M., Sobek, S., 2018. Spatially Resolved Measurements of CO_2 and CH_4 Concentration and Gas-Exchange Velocity Highly Influence Carbon-Emission Estimates of Reservoirs. Environ. Sci. Technol. 52, 607-615. https://doi.org/10.1021/acs.est.7b05138.

Peter, H., Singer, G.A., Preiler, C., Chifflard, P., Steniczka, G., Battin, T.J., 2014. Scales and drivers of temporal pCO_2 dynamics in an Alpine stream. J. Geophys. Res.-Biogeosci. 119, 1078-1091. https://doi.org/10.1002/2013jg002552.

Qian, J.T., Wu, Q.X., Aa, Y.L., Hou, Y.L., Han, G.L., Tu, C.L., 2017. Partial pressure of CO_2 and CO_2 outgassing fluxes of Sancha River. China Environ. Sci. 37, 2263-2269 (in chinese).

Ran, X.B., Liu, S., Liu, J., Zang, J.Y., Che, H., Ma, Y.X., Wang, Y.B., 2016. Composition and variability in the export of biogenic silica in the Changjiang River and the effect of Three Gorges Reservoir. Sci. Total Environ. 571, 1191-1199. https://doi.org/10.1016/j.scitotenv.2016.07.125.

Raymond, P.A., Caraco, N.F., Cole, J.J., 1997. Carbon dioxide concentration and atmospheric flux in the Hudson River. Estuaries. 20, 381-390. https://doi.org/10.2307/1352351.

Raymond, P.A., Hartmann, J., Lauerwald, R., Sobek, S., McDonald, C., Hoover, M., Butman, D., Striegl, R., Mayorga, E., Humborg, C., Kortelainen, P., Durr, H., Meybeck, M., Ciais, P., Guth, P., 2013. Global carbon dioxide emissions from inland waters. Nature. 503, 355-359. https://doi.org/10.1038/nature12760.

Richter, B.D., Postel, S., Revenga, C., Scudder, T., Lehner, B., Churchill, A., Chow, M., 2010. Lost in development's shadow: the downstream human consequences of dams. Water Altern. 3, 14-42.

Samanta, S., Dalai, T.K., Pattanaik, J.K., Rai, S.K., Mazumdar, A. Dissolved inorganic carbon (DIC) and its $\delta^{13}C$ in the Ganga (Hooghly) River estuary, India: Evidence of DIC generation via organic carbon degradation and carbonate dissolution. 2015 Geochim. Cosmochim. Acta. https://doi.org/165226-248. 10.1016/j.gca.2015.05.040.

Shi, W., Chen, Q., Yi, Q., Yu, J., Ji, Y., Hu, L., Chen, Y., 2017. Carbon Emission from Cascade Reservoirs: Spatial Heterogeneity and Mechanisms. Environ. Sci. Technol. 51, 12175-12181. https://doi.org/10.1021/acs.est.7b03590.

Sun, Z.G., Zhang, L., Duan, Z.D., 2013. The quantity and distribution of reservoir projects in China. China water resources. 10-11. https://doi.org/10.3969/j.issn.1000-1123.2013.07.006 (in Chinese).

Tang, W.K., Tao, Z., Gao, Q.Z., Mao, H.R., Jiang, G.H., Jiao, S.L., Zheng, X.B., Zhang, Q.Z., Ma, Z.W., 2014. Biogeochemical processes of the major ions and dissolved inorganic carbon in the Guijiang River. Environ Sci. 6, 2099-2107 (in chinese).

Teodoru, C.R., Del Giorgio, P.A., Prairie, Y.T., St-Pierre, A., 2013. Depositional fluxes and sources of particulate carbon and nitrogen in natural lakes and a young boreal reservoir in Northern Québec. Biogeochemistry. 113, 323-339. https://doi.org/10.1016/10.1007/s10533-012-9760-x.

Umetrics, User Guide SIMCA-+ 12, Umetrics, 2008.

Tranvik, L.J., Downing, J.A., Cotner, J.B., Loiselle, S.A., Striegl, R.G., Ballatore, T.J., Dillon, P., Finlay, K., Fortino, K., Knoll, L.B., 2009. Lakes and reservoirs as regulators of carbon cycling and climate. Limnology and Oceanography. 54, 2298-2314. https://doi.org/10.4319/lo.2009.54.6_part_2.2298.

Van, C.P., Maavara, T., 2016. Rivers in the Anthropocene: Global scale modifications of riverine nutrient fluxes by damming. Ecol. Hydrobiol. 16(2), 106-111. https://doi.org/10.1016/j.ecohyd.2016.04.001.

Vuorio, K., Meili, M., Sarvala, J., 2006. Taxon-specific variation in the stable isotopic signatures ($\delta^{13}C$ and $\delta^{15}N$) of lake phytoplankton. Freshwater Biology. 51, 807-822. https://doi.org/10.1111/j.1365-2427.2006.01529.x.

Wang, S.L., Yeager, K.M., Wan, G.J., Liu, C.Q., Liu, F., Lü, Y.C., 2014. Dynamics of CO_2 in a karst catchment in the southwestern plateau, China. Environmental Earth Sciences. 73(5): 2415-2427. https://doi.org/10.1007/s12665-014-3591-0.

Wang, B.L., Zhang, H.T., Liang, X., Li, X.D., Wang, F.S., 2019a. Cumulative effects of cascade dams on river water cycle: Evidence from hydrogen and oxygen isotopes. J. Hydrol. 568, 604-610. https://doi.org/10.1016/j.jhydrol.2018.11.016.

Wang, F.S., Lang, Y.C., Liu, C.Q., Qin, Y., Yu, N.X., Wang, B.L., 2019b. Flux of organic carbon burial and carbon emission from a large reservoir: implications for the cleanliness assessment of hydropower. Sci. Bull. https://doi.org/10.1016/j.scib.2019.03.034.

Wang, B.L., Liu, C.Q., Wang, F., Liu, X.L., Wang, Z. L., 2014. A decrease in pH downstream from the hydroelectric dam in relation to the carbon biogeochemical cycle. Environmental Earth Sciences. 73, 5299-5306. https://doi.org/10.1007/s12665-014-3779-3.

Wang, W.F., Li, S.L., Zhong, J., Li, C., Yi, Y.B., Chen, S.N., Ren, Y.M., 2019c. Understanding transport and transformation of dissolved inorganic carbon (DIC) in the reservoir system using $\delta^{13}C_{DIC}$

and water chemistry. J. Hydrol. 574, 193-201. https://doi.org/10.1016/j.jhydrol.2019.04.036.

Watkins, L., McGrattan, S., Sullivan, P.J., Walter, M.T., 2019. The effect of dams on river transport of microplastic pollution. Sci. Total Environ. 664, 834-840. https://doi.org/10.1016/j.scitotenv.2019.02.028.

Yang, S.L., Zhang, J., J. Zhu, Smith, J.P., Dai, S.B., Gao, A., Li, P., 2005. Impact of dams on Yangtze River sediment supply to the sea and delta intertidal wetland response. J. Geophys. Res. 110. https://doi.org/10.1029/2004jf000271.

Zeng, J., Han, G.L., Zhu, J.M., 2019. Seasonal and Spatial Variation of Mo Isotope Compositions in Headwater Stream of Xijiang River Draining the Carbonate Terrain, Southwest China. Water. 11, 1076. https://doi.org/10.3390/w11051076.

Zhang, Y., Wu, Z., Liu, M., He, J., Shi, K., Zhou, Y., Wang, M., Liu, X., 2015. Dissolved oxygen stratification and response to thermal structure and long-term climate change in a large and deep subtropical reservoir (Lake Qiandaohu, China). Water Res. 75, 249-58. https://doi.org/10.1016/j.watres.2015.02.052.

Zhao, Y., Liu, P.F., Rui, J.P., Cheng, L., Wang, Q., Liu, X., Yuan, Q., 2019. Dark carbon fixation and chemolithotrophic microbial community in surface sediments of the cascade reservoirs, Southwest China. Sci. Total Environ. 134316. https://doi.org/10.1016/j.scitotenv.2019.134316.

Zhong, J., Li, S.L., Cai, H.M., Yue, F.J., Tao, F.X., 2018a. The Response of Carbon Geochemistry to Hydrological Events within an Urban River, Southwestern China. Geochem int. 56, 462-473. https://doi.org/10.1134/s0016702918050099.

Zhong, J., Li, S.L., Liu, J., Ding, H., Sun, X.L., Xu, S., Wang, T.J., Ellam, R.M., Liu, C.Q., 2018b. Climate variability controls on CO_2 consumption fluxes and carbon dynamics for monsoonal Rivers: Evidence from Xijiang River, Southwest China. J. Geophys. Res.-Biogeosci. 123, 2553-2567. https://doi.org/10.1029/2018jg004439., .

Zhong, J., Li, S.L., Tao, F.X., Yue, F.J., Liu, C.Q., 2017. Sensitivity of chemical weathering and dissolved carbon dynamics to hydrological conditions in a typical karst river. Sci Rep. 7, 42944. https://doi.org/10.1038/srep42944.

Zhou, Y.L., Guo, S.L., Chang, F.J., Liu, P., Chen, A.B., 2018. Methodology that improves water utilization and hydropower generation without increasing flood risk in mega cascade reservoirs. Energy. 143, 785-796. https://doi.org/10.1016/j.energy.2017.11.035.

Table 1. The basic characteristics of the studied reservoirs. The classification of up-stream, mid-stream and down-stream and data from hydrological monitoring stations are derived from the Guizhou meteorological bureau and a previous study (Liang et al., 2017).

Reservoir	Hongjiadu (HJD)	Dongfeng (DF)	Suofengying (SFY)	Wujiangdu (WJD)	Silin (SL)	Pengshui (PS)	Yinpan (YP)
Year of construction	2004	1994	2002	1979	2006	2003	2007
Catchment area (km^2)	9900	18161	21862	27790	48558	69000	74910
Elevation (m)	1140	970	835	760	440	293	215
Approximate water depth (m)	70 - 110	70 - 110	60 - 80	70 - 110	60 - 80	60 - 80	60 - 80
Average annual runoff (10^8 m^3)	48.88	108.80	134.66	158.31	267.74	409.97	435.20
Total storage (10^8 m^3)	49.25	8.63	1.57	21.4	15.93	11.68	3.2
Regulation storage (10^8 m^3)	33.61	4.9	0.85	13.5	3.17	5.18	0.37
Regulation mode	Multi-year	Seasonal	Daily	Seasonal	Monthly	Monthly	Daily
HRT (day)	368	29	4	49	22	10	3
Storage coefficient (%)	68.8	4.5	0.6	8.5	1.2	1.3	0.1
Location, Annual mean air temperature (℃)/ precipitation (mm)	Upstream, 14.1/965			Mid-stream, 15.5/1057		Downstream, 17.4/1125	

Table 2: Environmental characteristics explaining the variability in DIC and $\delta^{13}C_{DIC}$ in the studied reservoirs, analysed using PLS with 3 components. Variable importance in projection (VIP) describes how much a variable contributes to explaining the Y variable DIC (mmol/L)/$\delta^{13}C_{DIC}$ (‰). Highly important variables have VIP>1.0 (marked in bold), moderately important variables have VIP 0.8-1.0 (marked in italics), and unimportant variables have VIP <0.8. Q^2 represents the predictive ability and R^2Y the explained variance. Coefficients and intercepts are analogous to the slopes and intercepts in an ordinary multiple linear regression. Combine the values of original R^2Y (<0.4) and Q^2 (<0.05), the study indicate that the mode is valid.

Model			**PLS**		
Components			**3**		
Q^2 (0.86/0.72)		R^2Y (0.91/0.84)		Y (DIC(mmol/L)/$\delta^{13}C_{DIC}$ (‰))	
Parameters	VIP	Coefficients	Parameters	VIP	Coefficients
Ta (°C)	**1.35 /1.45**	0.40/-0.62	Depth (m)	*0.92/0.93*	0.14/0.15
pH	**1.26/1.21**	-0.33/0.41	DOC (mg/L)	*0.87*/0.43	0.38/0.14
Chl (μg/L)	*0.91*/**1.22**	-0.10/0.33	Tw (°C)	0.44/0.52	0.003/0.02
DO (mg/L)	**1.13**/0.73	-0.33/0.02			
HRT (day)	*0.85*/**1.05**	-0.20/0.08			
Intercept			0.02/0.06		

Figure captions

Fig. 1. Sampling sites of the river- reservoir system in the Wujiang River, See Table 1 for sites name and abbreviations of the reservoirs; the inset shows the location of the catchment in China with the Wujiang watershed shown as a red line.

Fig. 2. Variations of carbon concentrations and stable isotope ratios in surface water along the

Wujiang River. DIC concentration (a), DOC concentration (b), $\delta^{13}C_{DIC}$ (c) and pCO_2 (d). The x-coordinate represents the surface water samples at sampling points from W1 to W29; W9 is a tributary of the Wujiang River. See Fig. 1 for the location of sampling sites.

Fig. 3. Depth profiles of DIC and $\delta^{13}C_{DIC}$ for seven reservoirs in the warm season (April to September) and the cold season (October to the next March).

Fig. 4. Relationship between Δ[DIC] and $\Delta[\delta^{13}C_{DIC}]$ in depth profiles from seven reservoirs. The four quadrants indicate different processes that influence Δ[DIC] and $\Delta[\delta^{13}C_{DIC}]$. The colour of the circle outline represents the site and the fill colour the depth. The quadrant BP/OG represents biological production and outgassing of CO_2 that results in a decrease of both Δ[DIC] and $\Delta[\delta^{13}C_{DIC}]$ (Alling et al., 2012; Kumar et al., 2019b). The quadrant CP represents calcite precipitation, which causes Δ[DIC] to decrease and $\Delta[\delta^{13}C_{DIC}]$ to increase (Samanta et al., 2015). The quadrant DC represents the degradation of organic carbon which causes an increase of both Δ[DIC] and $\Delta[\delta^{13}C_{DIC}]$ (Wang et al., 2019c). The quadrant CD represents calcite dissolution, which causes Δ[DIC] to increase and $\Delta[\delta^{13}C_{DIC}]$ to decrease (Abril et al., 2003). The dashed red lines is the linear fitting of the Δ[DIC] and $\Delta[\delta^{13}C_{DIC}]$.

Fig. 5. Relationship between changes in Δ [DIC] (%) and Δ $[\delta^{13}C_{DIC}]$ (%) and the quotient of Ta/ HRT for lakes from this study and the literature (see text). (a) Relationships of Ta/HRT versus Δ [DIC] (%), (b) Relationships of Ta/HRT versus Δ $[\delta^{13}C_{DIC}]$ (%). The dashes black lines in (a) and (b) represent the theoretical curve corresponding to HRT under a certain average Ta and the theoretical curve corresponding to Ta under a HRT, respectively. Overall, Ta and HRT are the two most important factors affecting river-lacustrine development.

Fig. 6. The conceptual diagram of DIC migration and transport across cascade reservoirs along the Wujiang River.

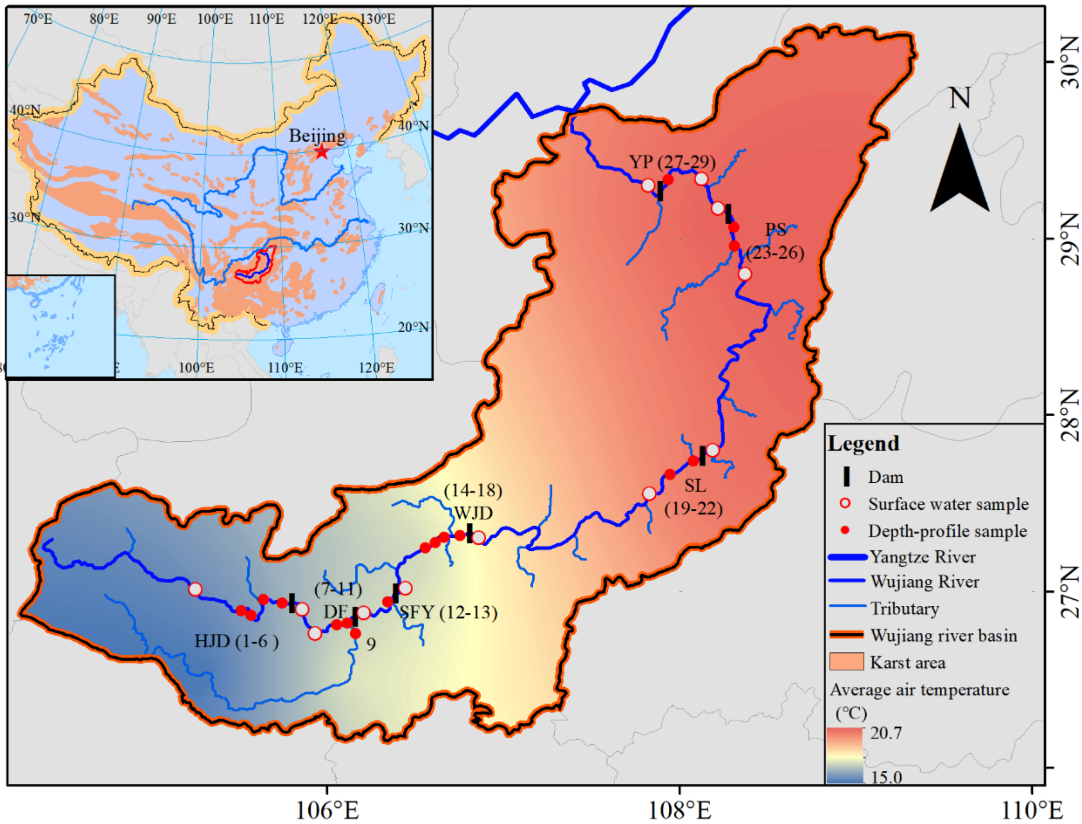
Beijing
YP (27-29)
PS
(23-26)
SL
(19-22)
(14-18)
WJD
(7-11)
DF
9
SFY (12-13)
HJD (1-6)
N
Legend
Dam
Surface water sample
Depth-profile sample
Yangtze River
Wujiang River
Tributary
Wujiang river basin
Karst area
Average air temperature
(°C)
20.7
15.0
106°E
108°E
110°E
27°N
28°N
29°N
30°N

Fig.1

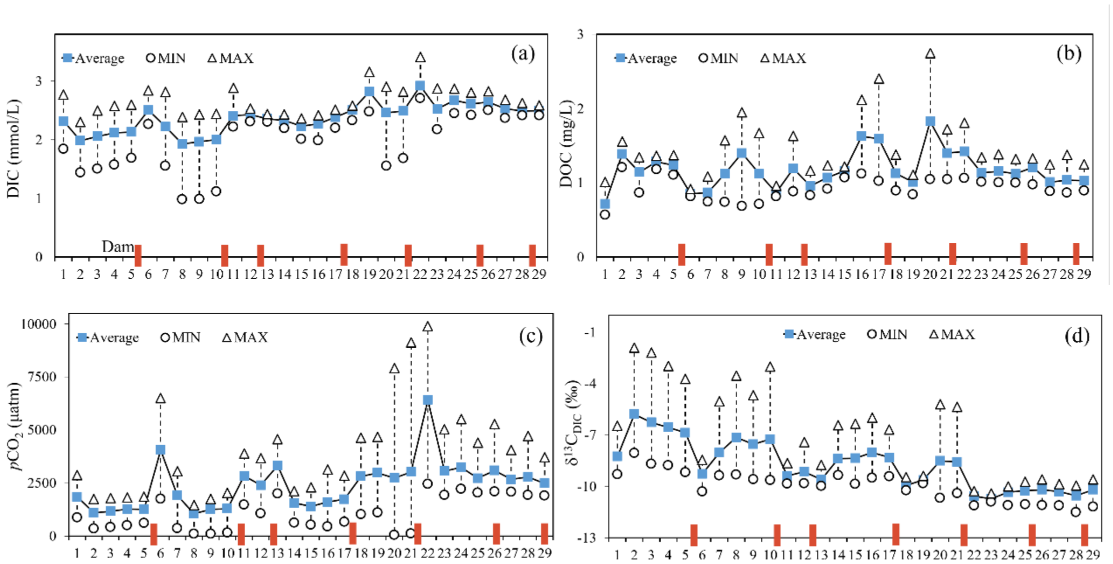
Average
MIN
MAX
(a)
(b)
(c)
(d)
DIC (mmol/L)
DOC (mg/L)
pCO$_2$ (μatm)
δ^{13}C$_{DIC}$ (‰)
Dam

Fig.2

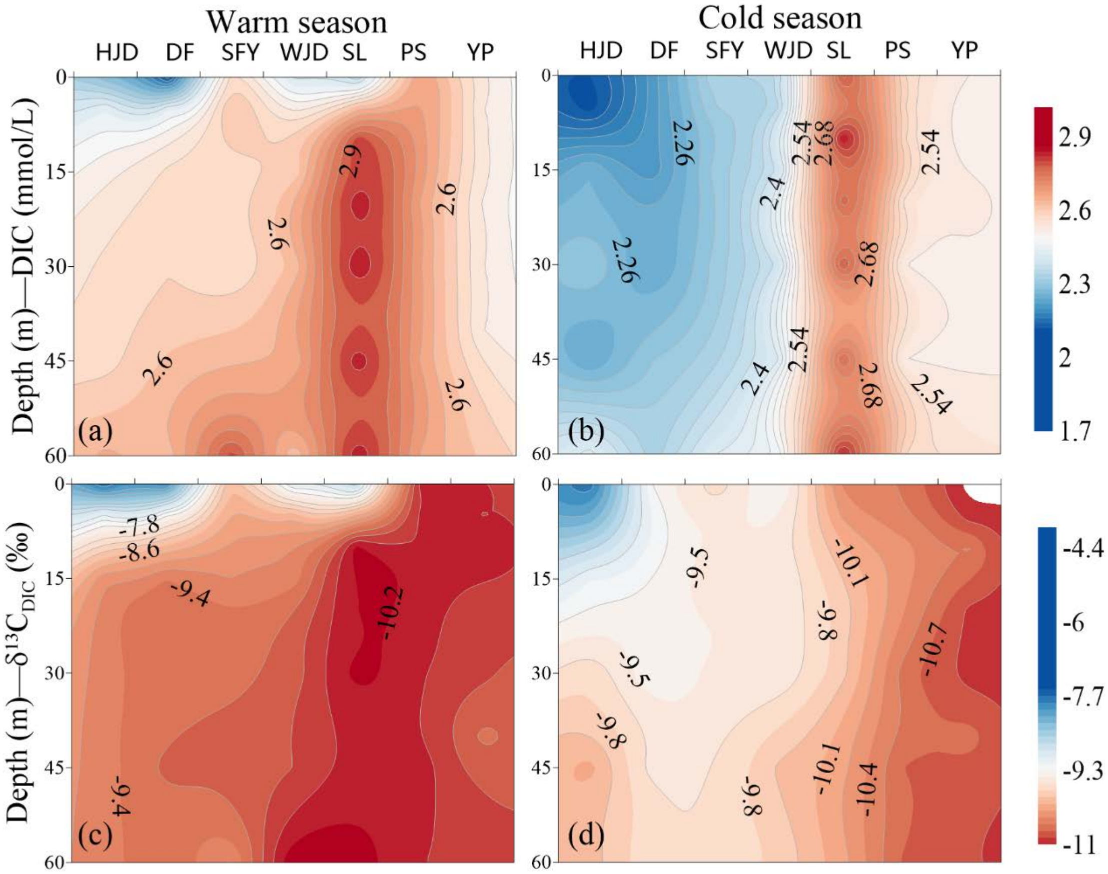
Warm season
Cold season
HJD DF SFY WJD SL PS YP
Depth (m)—DIC (mmol/L)
Depth (m)—$\delta^{13}C_{DIC}$ (‰)
(a)
(b)
(c)
(d)
2.9
2.6
2.3
2
1.7
-4.4
-6
-7.7
-9.3
-11

Fig.3

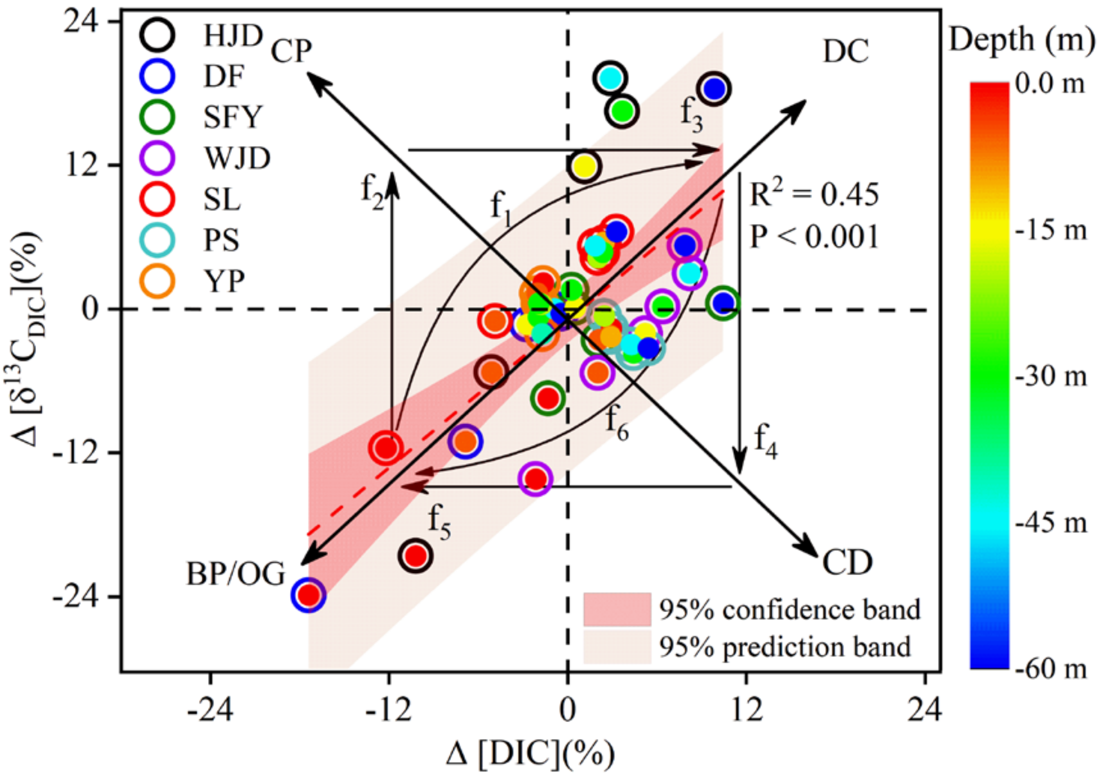
HJD
DF
SFY
WJD
SL
PS
YP
CP
DC
CD
BP/OG
f1
f2
f3
f4
f5
f6
$R^2 = 0.45$
$P < 0.001$
95% confidence band
95% prediction band
Depth (m)
0.0 m
-15 m
-30 m
-45 m
-60 m
$\Delta [\delta^{13}C_{DIC}](\%)$
$\Delta [DIC](\%)$

Fig.4

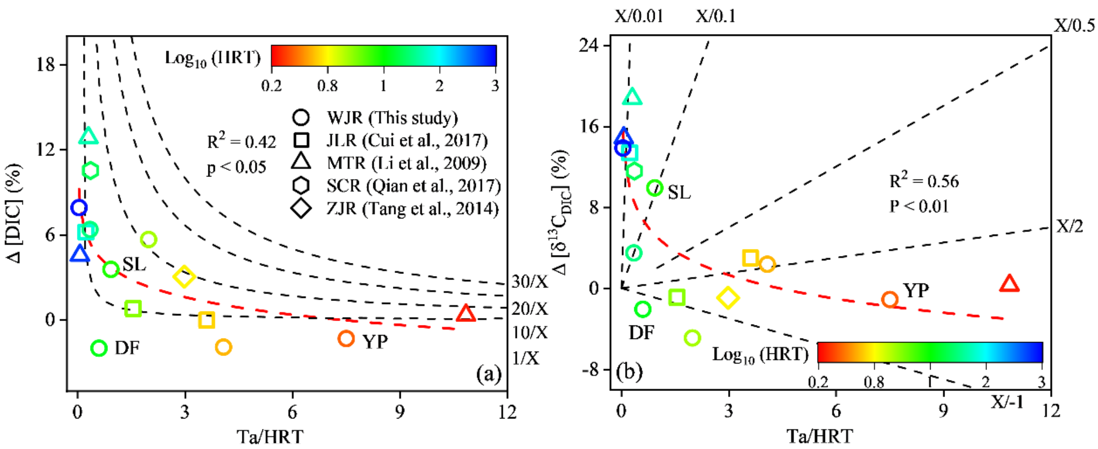
Log_{10} (HRT)
WJR (This study)
JLR (Cui et al., 2017)
MTR (Li et al., 2009)
SCR (Qian et al., 2017)
ZJR (Tang et al., 2014)
$R^2 = 0.42$
$p < 0.05$
SL
DF
YP
30/X
20/X
10/X
1/X
(a)
Δ [DIC] (%)
Ta/HRT
X/0.01
X/0.1
X/0.5
X/2
X/-1
$R^2 = 0.56$
$P < 0.01$
(b)
$\Delta [\delta^{13}C_{DIC}]$ (%)
Ta/HRT

Fig.5

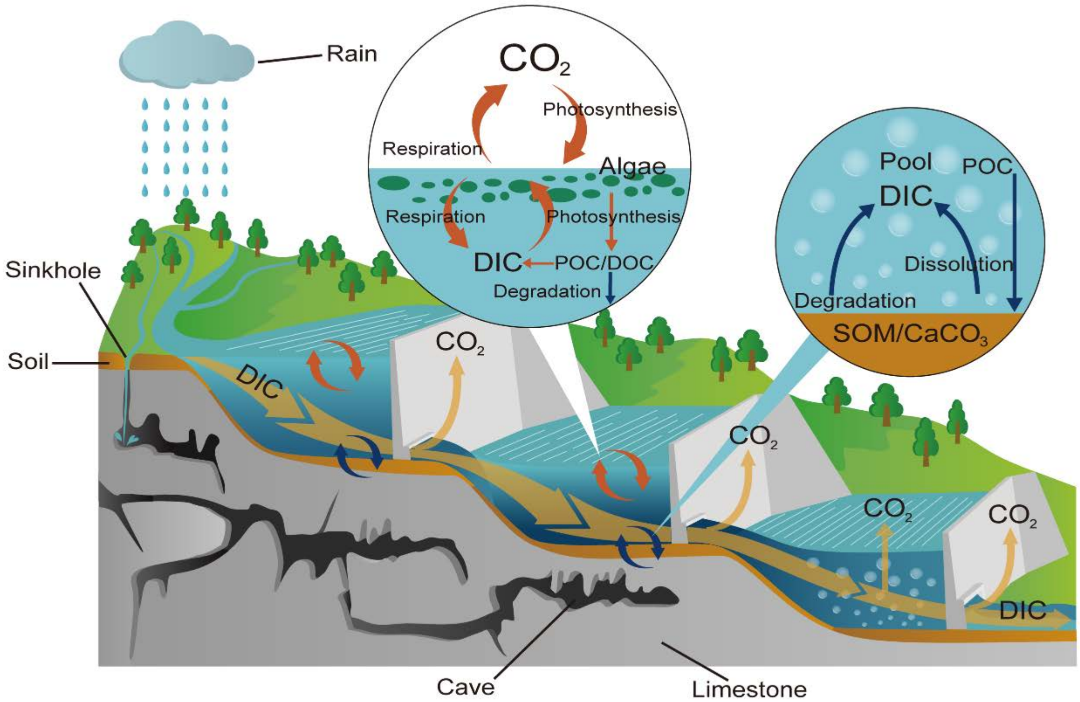
Rain
CO_2
Photosynthesis
Respiration
Algae
Respiration
Photosynthesis
DIC
POC/DOC
Degradation
Pool
POC
DIC
Dissolution
Degradation
SOM/$CaCO_3$
Sinkhole
Soil
DIC
CO_2
CO_2
CO_2
CO_2
DIC
Cave
Limestone

Fig.6